

Electronic Supplementary Information:

Synthesis and Characterization of Photoelectrochemical and Photovoltaic $\text{Cu}_2\text{BaSnS}_4$ Thin Films and Solar Cells

Jie Ge and Yanfa Yan

Department of Physics and Astronomy & Wright Center for Photovoltaics Innovation and Commercialization, the University of Toledo, Toledo, Ohio, 43606, United States.

* Email: Jie.Ge@UToledo.Edu; Yanfa.Yan@UToledo.Edu.

Experimental Section

Materials synthesis and device fabrication: $\text{Cu}_2\text{BaSnS}_4$ (CBTS) precursor films were deposited on commercial FTO glasses (TEC 15, NSG) and fused silica substrates by co-sputtering Cu, SnS and BaS targets (3 in.). The substrate temperature was kept at 150 °C during co-sputtering. During co-sputtering, the pressure inside the vacuum chamber was maintained at 1.5 mTorr. The composition of film precursors was controlled by varying the radio-frequency power for each target: 44/46/48 W for Cu, 43 W for SnS, and 110 W for BaS. The co-sputtered precursor films were then annealed in sulfur vapor at 560 °C for 30 min to yield the trigonal CBTS phase. The post-annealing was carried out in a tube furnace (Carbolite Gero) under the argon ambient of 400-500 Torr. The sulfurized CBTS films were dipped in a 1 M KCN aqueous solution for 1 min, followed by deionized water and methanol rinsing for 2 min and drying with nitrogen.

For Pt surface catalyzation, all the CBTS photoelectrodes were immersed in 0.1 M sodium sulfate aqueous solution containing 1 mM chloroplatinic acid and the photo-assisted electrodeposition was performed with a constant potential of -0.4 V *versus* Ag/AgCl (1M KCl) for 2 min.

For photovoltaic (PV) applications, CdS buffers were deposited by RF sputtering (50 W) of a CdS target (2 in.) at room temperature or 150 °C for 5–7 min in a pure Ar environment (10 mTorr). The resistive and conductive ZnO bilayers were deposited by RF sputtering undoped ZnO and aluminum-doped ZnO targets at room temperature with an aperture mask with the area of 0.08 cm², defining the active area of CBTS solar cells.

Film characterization: X-ray diffraction (XRD) data were collected using a Rigaku Ultima III diffractometer with Cu $K\alpha$ lines (0.15418 nm) in Bragg-Brentano θ - 2θ scans, with the Cu source operated at 40 kV and 44 mA electron excitation current. Confocal Raman spectroscopy was carried out using a 632.8 nm laser (HORIBA Scientific), with the Raman shift calibrated by the single crystal Si at 520.4 cm⁻¹. The optical transmittance spectra of CBTS thin films were measured by an ultraviolet-visible (UV-Vis) spectrophotometer (PerkinElmer Lambda 1050). The composition of our CBTS thin films were characterized by energy dispersive X-ray spectroscopy (EDX) equipped in a cold-field-emission scanning electron microscope (FE-SEM) (Hitachi S4800 FE-SEM). X-ray Photoelectron Spectroscopy (XPS) was conducted using a PHI Quantum 2000 spectrometer

fitted with the monochromatic Al K α X-rays (1486.6 eV). Ar⁺ beam (200 eV) sputtering for 936 s was employed as needed to remove the contaminants (~10 nm) on the CBTS film surface. XPS data fits were done using the software of CasaXPS.

Device Testing: photoelectrochemical (PEC) measurements were carried out using potentiostat (ModuLab XM ECS Electrochemical Test System, Ametek Scientific Instruments) and the standard 3-electrode cell configuration using a Ag/AgCl (1 M KCl) reference electrode with a platinum wire as the counter electrode. A 300 W xenon lamp was used as the light source. The effective area of the photocathodes was defined by using epoxy (HYSOL 9462) to cover the sample edges and was determined by the software ImageJ. A neutral electrolyte solution of 0.5 M sodium sulfite and 0.5 M monobasic potassium phosphate was used for all the PEC and Mott-Schottky (MS) measurements. Impedance spectroscopy (IS) and capacitance-voltage (CV) measurements in dark of CBTS based PEC electrodes and PV solar cells were performed using the potentiostat equipped with a frequency analyzer module. A liquid helium cryostat was used for the low temperature IS and CV tests of the PV cells. The simulation of IS data was run using the software of ZSim 3.3d (EChem Software).

The spatial defect distribution of CBTS ($N_{CV} - \langle x \rangle$) can be derived from the CV profiles based on the relation

$$\langle x \rangle = \frac{A \epsilon_0 \epsilon_r}{C} \quad \text{vs.} \quad N_{CV} = -\frac{2}{A^2 e \epsilon_0 \epsilon_r} \left[\frac{d(C^{-2})}{dV} \right]^{-1}$$

where $\langle x \rangle$ is the profiling distance measured from the junction, A is the cell area, e is elemental electron charge, ϵ_0 is the vacuum dielectric constant, and ϵ_r is the relative dielectric constant of CBTS. Herein, we tentatively take $\epsilon_r \approx 5.4$.

Table S1. Calculated values of circuit elements of the equivalent circuit models developed for the measured complex impedance data of the CBTS PEC solar cell (Sample-C),^a shown in Figure 5a.

	R_s ($\Omega \cdot \text{cm}^2$)	C_{sc} ($\text{nF} \cdot \text{cm}^{-2}$)	R_{sc} ($\Omega \cdot \text{cm}^2$)	C_H ($\text{nF} \cdot \text{cm}^{-2}$)	R_{CT} ($\Omega \cdot \text{cm}^2$)	Warburg, Y_0 ($\text{S} \cdot \text{sec}^{0.5}$)
Model-1	41.49	2.857	141.3			0.994×10^{-3}
Model-2	46.13	3.042	147.5	366300	2936	2.564×10^{-3}

^a Sample-C indicates the CBTS film prepared by co-sputtering from Cu (46 W), SnS (43 W), and BaS (110 W) targets.

Table S2. Calculated values of circuit elements of the equivalent circuit model developed for the measured complex impedance data of the CBTS PV solar cell shown in Figure 7a (Sample-C).^a

Bias (V)	-0.6	-0.4	-0.2	0.0	0.2	0.4	0.6	0.8	1.0
R_s ($\Omega \cdot \text{cm}^2$)	19.3	19.5	20.4	18.3	19.4	19.2	19.0	19.0	19.0
C_{sc} ($\text{nF} \cdot \text{cm}^{-2}$)	7.20	7.48	7.51	7.01	7.84	8.05	8.61	8.34	8.30
R_{sc} ($\Omega \cdot \text{cm}^2$)	836.0	637.9	765.3	673.3	729.1	667.6	595.6	557.8	264.8
Y_1 ($\text{S} \cdot \text{sec}^n \cdot \text{cm}^{-2}$)	706.3	3375	2500	2612.5	3375	233.3	1275	1500	2837.5
n_1	0.85	0.511	0.8	0.553	0.642	0.666	0.707	0.772	0.586
C_1 ($\text{nF} \cdot \text{cm}^{-2}$) ^b	187.5	19.1	600	40.5	150	127.5	118.3	245	64.8
R_1 ($\Omega \cdot \text{cm}^2$)	9587	16740	16600	27870	13770	16190	31390	18240	21050
Y_2 ($\text{S} \cdot \text{sec}^n \cdot \text{cm}^{-2}$)	735	0.25	2862.5	815	2575	587.5	427.5	281.3	133.8
n_2	0.57	1.0	0.8	0.708	0.645	0.732	0.764	0.801	0.80
C_2 ($\text{nF} \cdot \text{cm}^{-2}$) ^c	11.7	0.25	448.8	35.1	81.3	36.8	34.9	32.5	10.0
R_2 ($\Omega \cdot \text{cm}^2$)	5631	55816	210.2	600.6	716.2	891.2	698.6	592.5	239.0
L ($\text{H} \cdot \text{cm}^2$)					89600	144.6	240.9	96.2	6.6
R ($\Omega \cdot \text{cm}^2$)					35904	252.2	6.9	670.2	0.001

^a Sample-C indicates the CBTS film prepared by co-sputtering from Cu (46 W), SnS (43 W), and BaS (110 W) targets.

^{b, c} the pseudo capacitances of the constant phase elements are derived from the expression $C_i =$

$$\frac{(Y_i R_i)^{\frac{1}{n_i}}}{R_i} \quad (i = 1, 2).$$

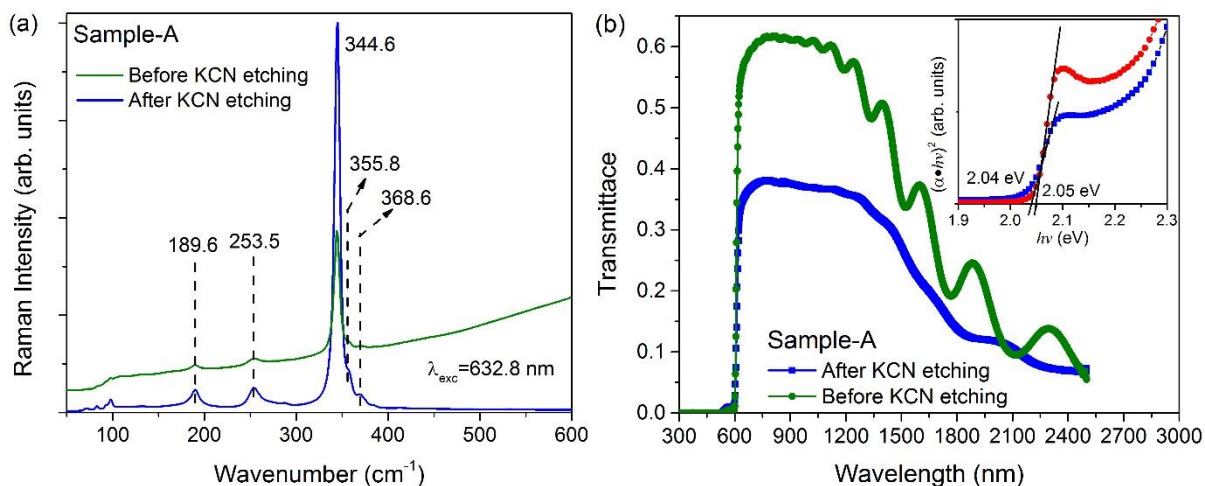


Figure S1 Raman scattering spectra (b), and optical transmittances and bandgap plots (c) of a sulfurized CBTS film (Sample-A) before and after the treatment in 1 M KCN aqueous solution for 1 min. Note: in the bandgap plots of panel (c) inset, hv —photon energy, and the absorption coefficient α was derived from the optical transmittance (T) and film thickness (t) based on the relation $\alpha = \frac{1}{t} \ln \frac{1}{T}$; Sample-A indicates the film prepared by co-sputtering from Cu (44 W), SnS (43 W), and BaS (110 W) targets.

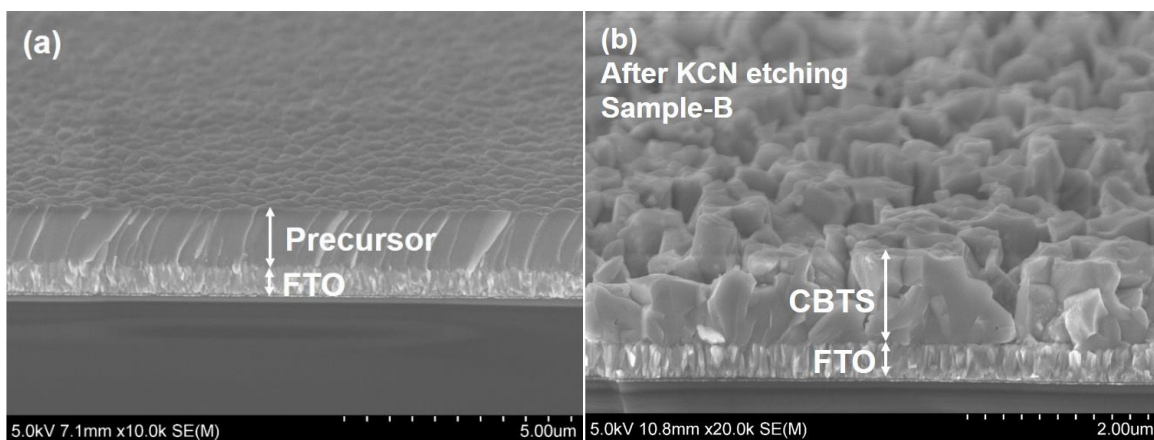


Figure S2. Cross-sectional SEM images of a precursor film deposited on a FTO substrate (a) and a sulfurized CBTS film (Sample-B) after KCN etching. Note: Co-sputtering time for precursor deposition is 75 min; Sample-B indicates the film prepared by co-sputtering from Cu (48 W), SnS (43 W), and BaS (110 W) targets.

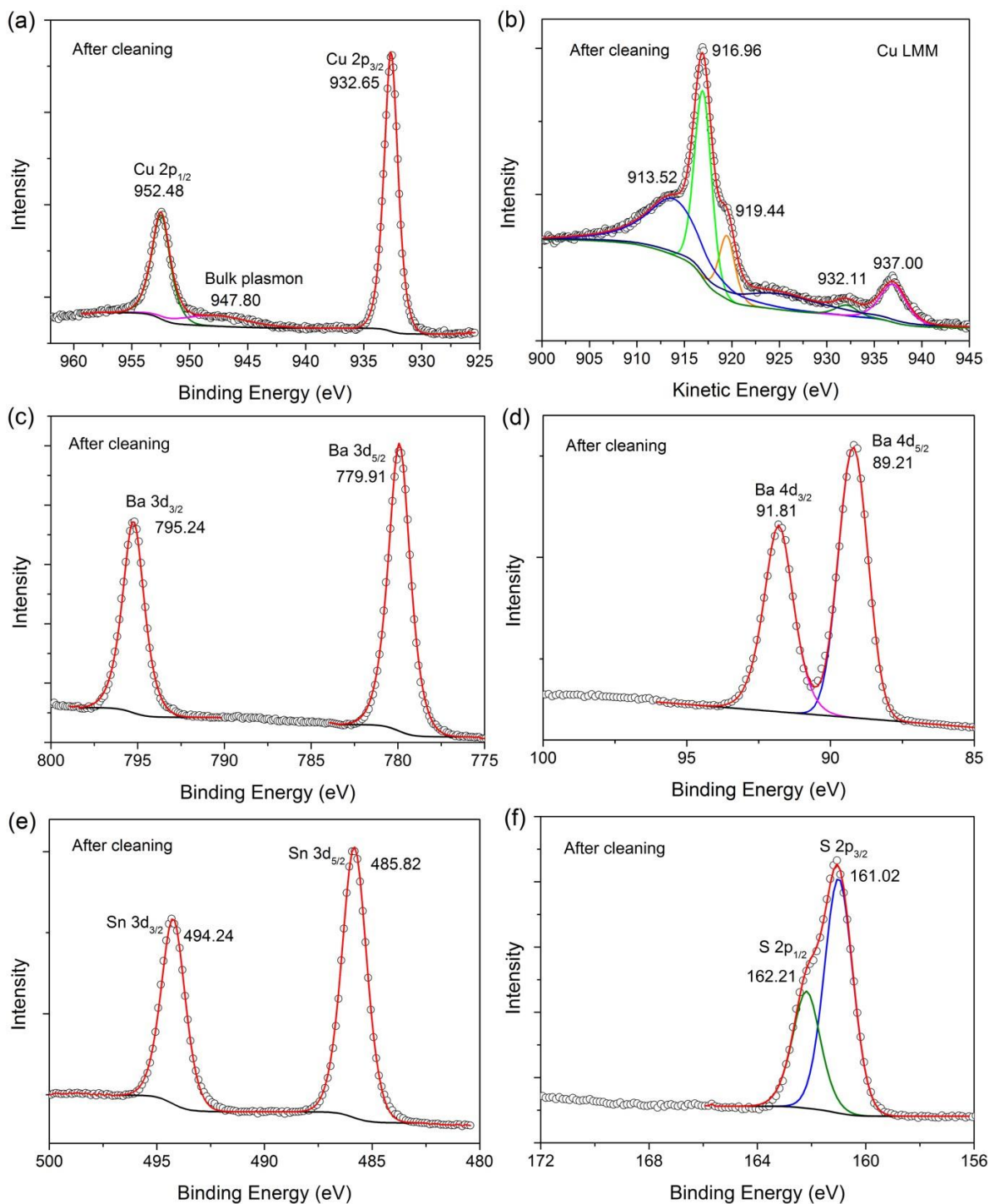


Figure S3. XPS spectra of a CBTS film (Sample-C) after subsequent surface cleaning using argon ion: (a) Cu 2p splitting peaks; (b) Cu LMM Auger peaks; (c) Ba 3d splitting peaks after Ar ion cleaning; (d) Ba 4d splitting peaks; (e) Sn 3d splitting peaks after Ar ion cleaning; (f) S 2p splitting peaks after Ar ion cleaning. Note: open symbols—raw data, black lines—Shirley background, colorful lines—fitted peaks, red lines—enveloping curves; Sample-C indicates the film prepared by co-sputtering from Cu (46 W), SnS (43 W), and BaS (110 W) targets.

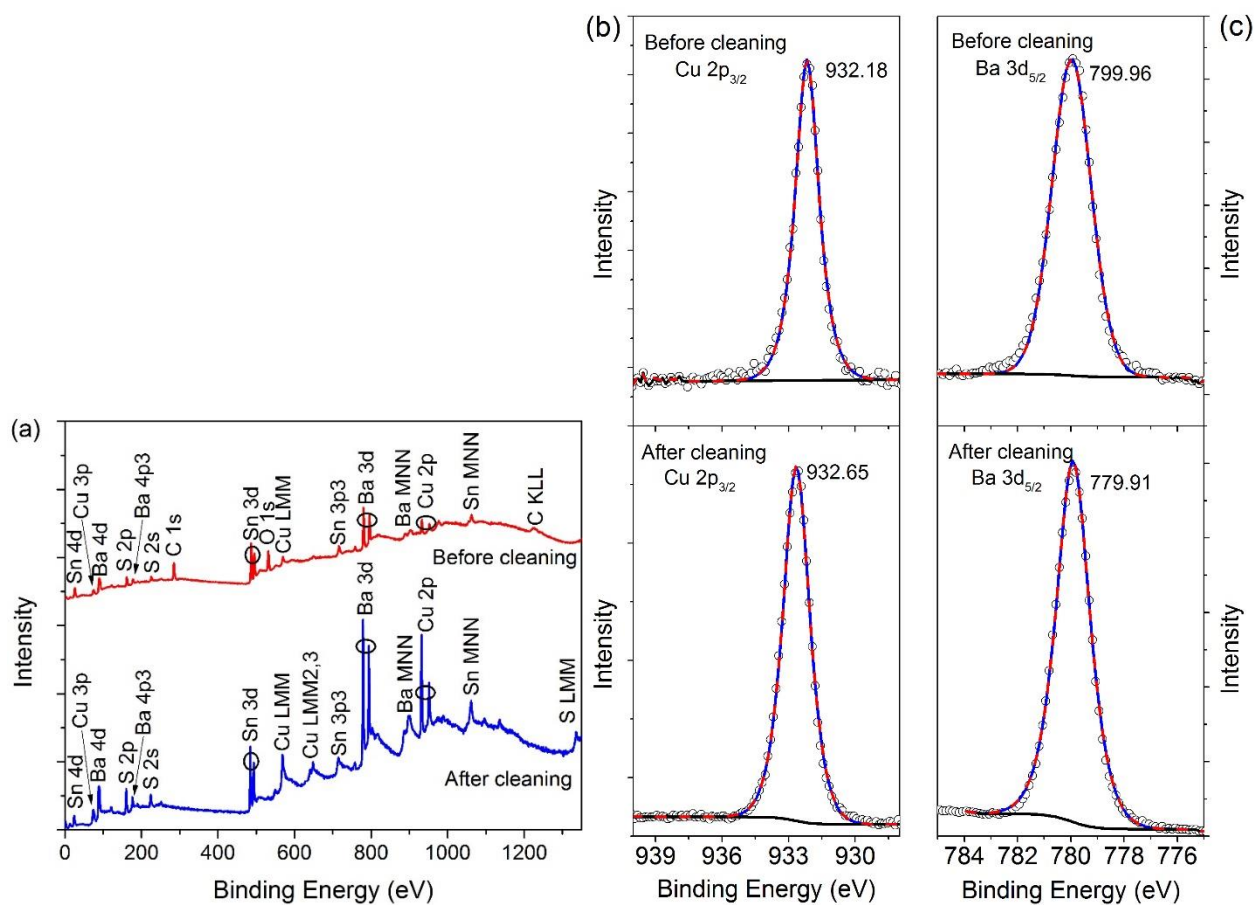


Figure S4. XPS spectra of a CBTS film (Sample-C) before and after surface cleaning using argon ion: (a) full survey spectra; (b) Cu 2p_{3/2} peaks; (c) Ba 3d_{5/2} peaks. Note: in panels (b) and (c), open symbols—raw data, black lines—Shirley background, blue lines—fitted peaks, red dash lines—enveloping curves; Sample-C indicates the film prepared by co-sputtering from Cu (46 W), SnS (43 W), and BaS (110 W) targets.

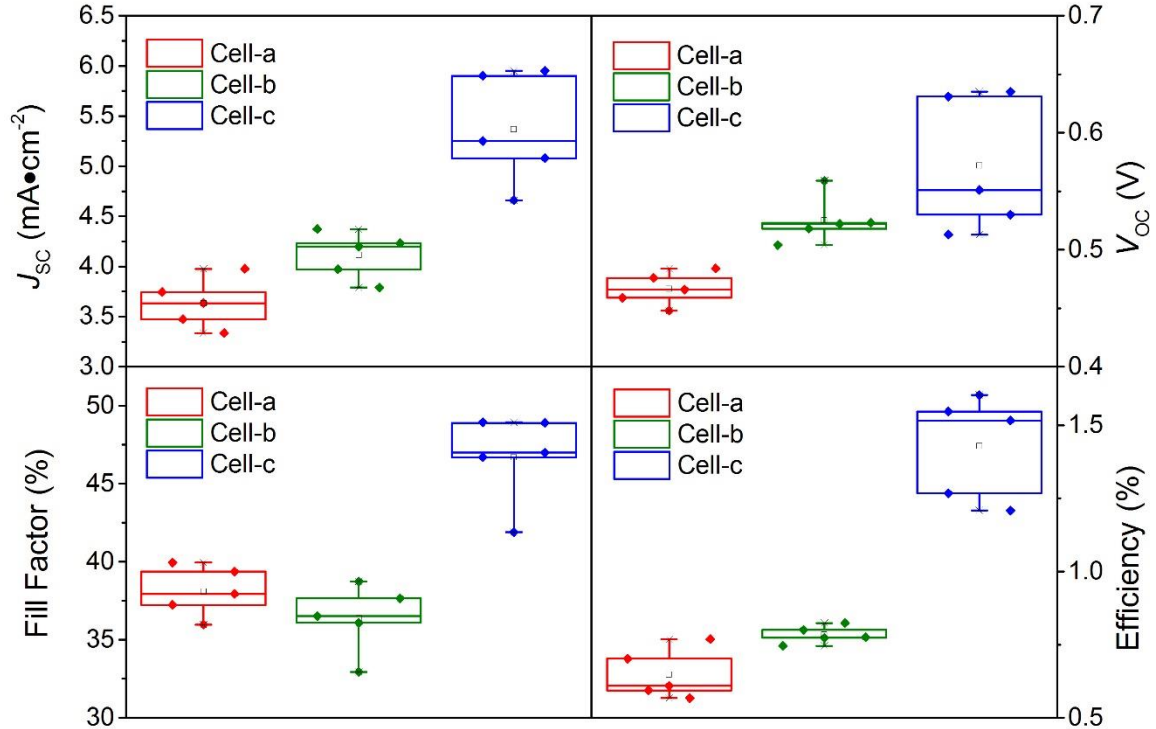


Figure S5. Solar cell parameters of the illuminated $J-V$ curves Figure 6: open circuit voltage (V_{oc}), short circuit current (J_{sc}), fill factor, and power conversion efficiency. The CBTS absorber film was prepared by co-sputtering from Cu (46 W), SnS (43 W), and BaS (110 W) targets.

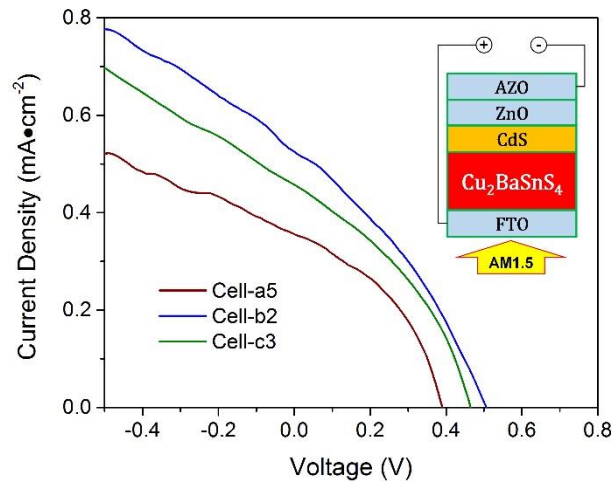


Figure S6. Light current-voltage ($J-V$) curves of CdS buffered CBTS solar cells (FTO/CBTS/CdS/ZnO/AZO) measured under AM 1.5G illumination from the FTO side: Cell-a5, the CdS buffer was sputtered in a pure Ar ambient at room temperature; Cell-b2, the finished device was annealed in air at 170 °C for 10 min on a hotplate; Cell-c3, the CdS buffer was sputtered in a pure Ar ambient at 150 °C; the CBTS absorber film was prepared by co-sputtering from Cu (46 W), SnS (43 W), and BaS (110 W) targets.